Chapter 14
Integration and Management Technique of Renewable Energy Resources in Microgrid

Hossein Shayeghi and Elnaz Shahryari

Abstract Ever increasing demand for electricity supply along with higher power quality and reliability, available fossil fuels restrictions and environmental pollutions led to aggregation of clean energy resources (distributed generations) and developing microgrids. Integration of distributed generations such as wind power and solar energy are challenging with various problems such as non-deterministic nature of available wind power and solar energy. On the other hand, power systems are subject to other uncertainties such as load and energy prices in day-ahead (DA) and balancing markets. Hence, intermittence could be highlighted as the main obstacle of distributed generations' aggregation which cause to imbalance charges set by uncertain market prices and accordingly economic losses. To this end, a comprehensive study should be performed to elaborate aforementioned issues. In this chapter, a stochastic model with the goal of profit maximization and imbalance cost minimization is presented. Unlike previous works, in the proposed model all existent uncertainties related to wind power, solar energy, load, day ahead and imbalance market prices altogether are considered by the means of scenario based investigations. In order to generate probable scenarios, uncertain parameters should be predicted. In this framework, a new method based on neural network theory is proposed for predicting wind speed and solar radiation. Afterwards, pumped-storage plant and demand response program are utilized as two complementary resources to compensate power imbalances. Storage devices are used as flexible resources to exchange power between low consumption—cheap hours and peak hours. Finally, to investigate efficiency of the proposed method two operating modes, namely coordinated and uncoordinated operation of clean energy resources, are assumed and testified on a test microgrid.

H. Shayeghi (✉) · E. Shahryari
Department of Technical Engineering, University of Mohaghegh Ardabili, Ardabil, Iran
e-mail: hshayeghi@gmail.com

E. Shahryari
e-mail: elnaz.shahryari@yahoo.com

N. Bizon et al. (eds.), *Energy Harvesting and Energy Efficiency*,
Lecture Notes in Energy 37, DOI 10.1007/978-3-319-49875-1_14

Keywords Clean energy resources · Uncertainty · Demand response · Microgrid · Pumped-storage power plant · Mathematical modeling · Wind power producer · Photovoltaic · Scenario generation

List of Symbols

Indices and numbers

S Set of scenarios
T Settlement time period

Parameters and constants

ρ_s	Probability of scenario s
$P^{W\,max}$	Maximum energy of wind turbine, kW
$P^{PV\,max}$	Maximum energy of PV system, kW
V^{UU}	Maximum charging capacity of storage, kW
V^{DU}	Minimum charging capacity of storage, kW
V^{UL}	Maximum discharging capacity of storage, kW
V^{DL}	Minimum discharging capacity of storage, kW
η_1	Percentage of demanded load reduction
η_2	Percentage of demanded load increase
Vf^U	Primary and ultimate energy value of upper reservoir, kW
Vf^L	Primary and ultimate energy value of bottom reservoir, kW
η	Operation efficiency of pumped-storage unit in pumping and generating mode
N	Number of the pumped-storage units
α	Factor of load recovery
β	Elasticity factor

Variables and parameters

$\pi_{DA,t,s}$	Day-ahead electricity price at time period t and output scenario s, $/MWh
$\alpha^{+}_{t,s}$	Overproduction imbalance price ratio at time period t and output scenario s
$\alpha^{-}_{t,s}$	Underproduction imbalance price ratio at time period t and output scenario s
P^{WPP}_{t}	Offered power by wind power producer in *t*th hour, kW
P^{PV}_{t}	Offered power by PV system in *t*th hour, kW
P^{PUMP}_{t}	Offered power by storage in *t*th hour, kW
D_t	Offered power by demand response in *t*th hour, kW
$P^{WPP}_{t,s}$	Real scheduled power of wind power in *S*th scenario and *t*th hour, kW
$P^{PV}_{t,s}$	Real scheduled power of PV system in *S*th scenario and *t*th hour, kW
$D_{t,s}$	Real scheduled demanded load in *S*th scenario and *t*th hour, kW

$g_{t,S}^{Pump}$ Discharge power output of storage in Sth scenario and tth hour s, kW
$d_{t,S}^{Pump}$ Pumping power of storage in Sth scenario and tth hour, kW

Integer variables

$t_{t,S}$ Binary variable to specify if the storage unit is capable to operate as a turbine or not in Sth scenario and tth hour
$u_{t,S}$ Number of units running in pumping mode in Sth scenario and tth hour
$y_{t,S}, z_{t,s}$ Number of start-ups and shut-downs in Sth scenario and tth hour

Abbreviation and Acronyms

DA Day-ahead
DG Distributed generation
DO Disjoint operation
MCP Marginal clearing price
MG Microgrid
MLP Multi-layer perceptron
MSE Mean square error
MT Micro turbine
NN Neural network
PV Photovoltaic
WT Wind turbine

14.1 Introduction

Recently, there is a strong attitude toward utilizing distributed generations (DGs) as the alternative to traditional ones. Distributed generations are small scale generation units such as small wind turbines (WTs), Photovoltaic (PV), fuel cells, and Micro turbines (MTs) which are installed close to the consumers [1]. Electricity cheapness, higher reliability and quality in providing power services and satisfying environmental concerns are the most important benefits of using DGs [2].

By aggregation of distributed generations, loads and energy storage devices a microgrid (MG) is formed [3] which can be operated in a grid-connected or islanding mode. Since, the output voltage and frequency of DGs are not regulated and on the other hand, these power sources have stochastic nature, their output is in DC or unregulated Ac form. This makes it necessary to connect and control output power of distributed generation units via power electronic converters [4, 5].

In the grid-connected mode, the main grid is responsible for regulating voltage and frequency of microgrid [6]. To reach this goal, the difference between generated and demanded power in the microgrid is calculated and then the main grid is responsible to hold balance in the microgrid. So, lack of main grid in islanding operating mode makes difficulties in microgrid control. The control method of microgrid in islanding mode should be able to regulate its voltage and frequency in order to maintain its dynamic stability at any time which can be performed by fast-response storage devices such as batteries. The second aim of microgrid controlling is to provide power balance between generation and consumption [7]. Therefore, an efficient power management method is required to make the most appropriate decision for various conditions of power sources, demanded load, electricity price and many other circumstances.

On the other hand, deregulation is new template of power industry which tries to reach a high level of competition between market participants, maximizing economic benefits, and also creating new options for consumers [8]. In deregulation template, electricity market price for each hour of future is determined by offers of consumers and power generators. By the way, because of non-deterministic nature of DGs, the amount of future generation for these units should be estimated by short term forecasting tools [9]. Various prediction methods have been presented in the literature such as artificial neural network [10], ANFIS [11] wavelet transform [12], Kalman filtering [13]. Also, researchers in [14] proposed a method to forecast two dependent parameters, load and market clearing price, simultaneously as a multi-input multi-output model.

Taking into account deregulation rules, wind and solar power producers submit their offers to the market while they are unaware of their exact production level. This leads to generation of unbalances between scheduled and delivered energy which should be compensated in balancing markets [15]. Prior to introduction of MG, various studies have been performed about DGs. For instance, in [16] wind and photovoltaic generations for supplying an office building are designed in such a way that annual costs of the overall system are minimized and economical and environmental profits are maximized. The effects of distributed generations on expansion of sub-transmission system is studied in [17] and all of fixed and variable costs of DGs are considered in mathematical formulation. A mixed-integer mathematical formulation is presented in [18] in order to determine the optimal offers of wind farm and storage unit in day-ahead market. In this formulation, market prices related to power imbalances are assumed to be known. Authors of [19] employed stochastic programming techniques to simulate participation of wind power and storage unit owners in day-ahead and ancillary service markets as an integrated self-schedule. Reference [20] proposed a new method to model wind power and storage unit while utilizing Value at Risk (VaR) of units to measure their operation. In [21] profit maximization and optimal bids for participation of wind farm and demand response are calculated. In the presented method marginal and imbalance prices are considered known and wind producer offering is improved by using demand response as a storing device.

Research studies prove that independent utilization of DG units in power system can lead to lots of difficulties. So, in order to solve these problems, microgrid concept has been presented [22]. According to above claims, many researches have been carried out to identify different aspects of microgrids. Considering uncertainties related to wind speed, solar irradiance and load, reference [23], focuses on integration of DG units in a microgrid to reach maximum profit. In [24], microgrid planning is done in such a way to achieve the least amount of cost and emission. In [25] a novel coordinated bidding strategy is addressed to aggregate multiple DGs and storage units and demand response as an independent power producer in the microgrid in order to increase their revenue in intra-day market. Stochastic coordination of distributed resources considering related uncertainties in an islanding microgrid is studied in [26]. This paper takes into account intermittencies related to load, wind and solar generation by a set of probable scenarios. Authors of [27] have performed the optimal energy management for microgrid as a multi-objective problem while considering uncertain nature of wind and solar power. In this paper an incentive based demand response program is proposed to cover power uncertainties which makes it possible for various kinds of residential, commercial and industrial consumers to participate in demand response program. An energy management system is suggested by [28] to determine the optimal operating point of wind turbines along with storage devices in a microgrid and minimize its cost and emissions while considering wind uncertainty. Reference [26] models operation of distributed energy sources in a microgrid as a stochastic mathematical model which utilizes various possible scenarios in order to cover load, wind and solar uncertainties. In [29], a matrix real coded genetic algorithm method is applied to optimize the operation of microgrid. In this study, energy storage system is used to manage uncertainties of PV.

In this chapter, bidding strategy of microgrid components are discussed in detail and a scenario generation process based on prediction errors is utilized to cover existing uncertainties. Also demand response and pumped-storage are utilized as both storage device and power generator to adjust power imbalances. Comprehensive description of the issue is provided in the following sections.

14.2 Problem Description

In this section background knowledge related to the power markets and role of pumped-storage and demand response participation in power markets are discussed.

14.2.1 Day-Ahead and Balancing Market

The market considered in this chapter is composed of two sub-markets with distinct planning horizons which are named day-ahead (DA) and balancing market. Most of

power is exchanged in day-ahead markets. The basis of this market is auctions in which power producers and consumers propose their hourly offers based on final predictions before termination time which happens at 10:00 am and lasts for 15 until 38 h. Finally by computing junction point of summated hourly demand and supply functions, the marginal clearing price (MCP) for each hour is calculated. This price is the minimum price which satisfies all purchase bids with enough accepted sell offers. The payment process in day-ahead market is to pay multiplication of real generation and marginal price for each hour.

The wind and solar power producers must predict their future generation for next day in order to participate in day-ahead power market, however due to uncertain nature of wind and solar, always there are differences between predicted value and the real one. So in order to reduce imbalances between demand and generation power, balancing markets are employed in real time horizon. Power imbalances which can be calculated by subtraction of cleared generated power from real value, are settled and fined in balancing market. If there is overproduction, it will be settled cheaper than marginal price. Controversy, if there is underproduction, it will be compensated more expensive than marginal price. If $\pi_{up,t}$ and $\pi_{down,t}$ represent the imbalance prices for excess and lack of produced power, respectively, it can be said that $\pi_{up,t} \leq \pi_{DA,t} \leq \pi_{down,t}$ and the revenue earned from this market at time t is calculated as below:

$$R(\Delta P) = \begin{cases} \pi_{up,t}\left(P_{Gen,t} - P_{Bid,t}\right) & if \quad P_{Gen,t} \geq P_{Bid,t} \\ \pi_{down,t}\left(P_{Bid,t} - P_{Gen,t}\right) & if \quad P_{Gen,t} < P_{Bid,t} \end{cases} \tag{14.1}$$

Here $P_{Gen,t}$ and $P_{Bid,t}$ represent the actual and submitted generation offer in day-ahead market, respectively. By supposing $\alpha_t^+ \leq 1$ and $\alpha_t^- \geq 1$ as the ratio between sell and buy imbalance prices to marginal prices, imbalance prices can be computed as below:

$$\pi_{up,t} = \alpha_t^+ \pi_{DA,t}, \quad \pi_{down,t} = \alpha_t^- \pi_{DA,t} \tag{14.2}$$

By replacing Eq. (14.2) with Eq. (14.1), imbalance revenue is rewritten as below:

$$R(\Delta P) = \begin{cases} \alpha_t^+ \pi_{DA,t}\left(P_{Gen,t} - P_{Bid,t}\right) & if \quad P_{Gen,t} \geq P_{Bid,t} \\ \alpha_t^- \pi_{DA,t}\left(P_{Bid,t} - P_{Gen,t}\right) & If \quad P_{Gen,t} < P_{Bid,t} \end{cases} \tag{14.3}$$

14.2.2 Role of Pumped-Storage Unit

The aim of power producers in construction of pumped-storage plant is to support uncertainty of wind and solar power generations and provide flexibility to power generators by this complementation. For example, suppose that wind or solar power producers face with an overproduction in real time operation, it means that the

generated power in real time is more than the power which they should provide. In this situation, the surplus power is saved by pumping water from bottom tank to the upper. Vice versa, if there is lack of generation, this shortage could be compensated by hydro turbine. In this condition, delivered power is accurate and equals to the cleared amount in market. However, it should be considered that this flexibility depends on the characteristics of pumped-storage unit, too.

14.2.3 Role of Demand Response

Demand response (DR) is a program which enables end-users to participate in electricity markets. In this procedure, consumers submit their demanded loads to the market. After clearing the day-ahead market, consumers are charged for their submitted bids and also the value of MCP and production of each generating unit is specified. This program enables end-users to propose their load reduction bids to the market and to be paid by MCP in the case of admission. Response of consumers to the market price is called elasticity. Higher amount of elasticity makes consumers to react well in response to power price changes. So when the electricity price is high, consumers can adjust themselves by reducing consumption.

Coordinated operation of DR and clean energy sources like wind and solar power, could cover uncertainties of wind and solar. For example, in peak hours consumers can decrease their consumption and compensate uncertainty of wind power and photovoltaic. On the other hand, applying flexible load helps in improving welfare of power producers and minimizing the penalties that they should pay to imbalance market resultant from their uncertain nature.

The overall process of this chapter to aggregate clean energy sources in a microgrid is depicted in Fig. 14.1 which shows the total stages step by step.

14.3 Modelling Uncertainties

A situation in which there is lack of accurate and detailed information about present or future conditions is called uncertainty. Power systems confront with two main types of uncertainties which caused by failure of generation units or by prediction errors. Failure of generation units leads to lack of production which can be compensated via spinning or non-spinning reserves; but uncertainties related to prediction accuracy is consisted of load, produced power and market price uncertainties for each hour of next day. In this chapter second type of uncertainties is studied which can be controlled with stochastic programming techniques. In this method, aforementioned uncertain parameters must be predicted at first, then a scenario generation process based on prediction error is utilized to generate probable values of stochastic parameters. Finally, in order to speed up computation a scenario reduction technique is employed. Each of these steps are explained in detail as follows.

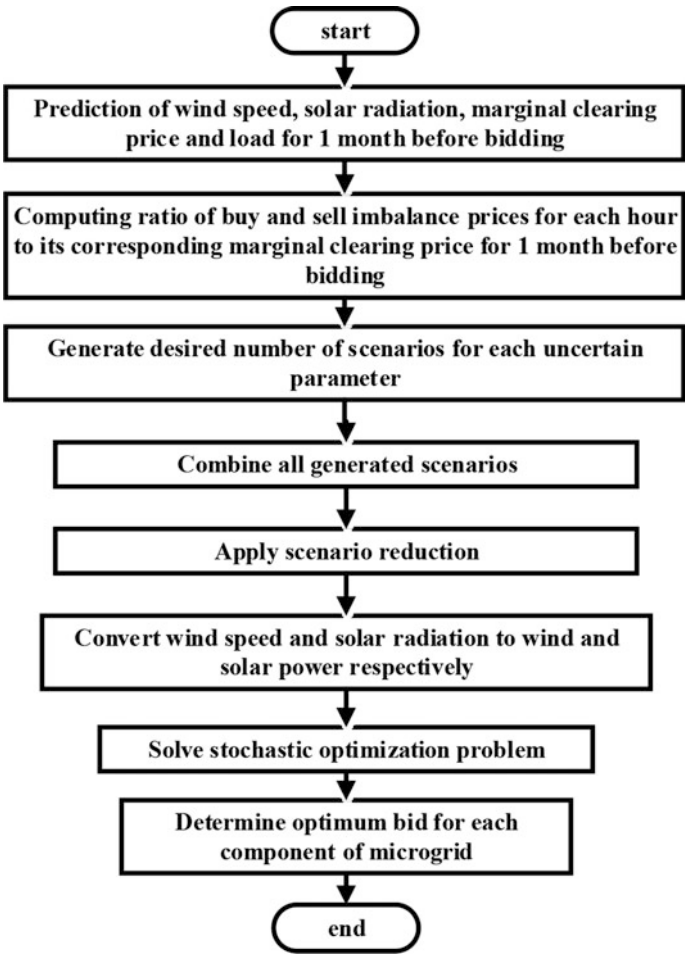

Fig. 14.1 Flowchart of aggregation of clean energy sources

14.3.1 Prediction Method

This chapter proposes a new technique for short term prediction of uncertain parameters based on neural network (NN). NN is a nonlinear modeling technique which is trained by historical data to specify the relation between input and output data. In this chapter, Multi-layer Perceptron (MLP) neural network with one hidden layer is utilized to do forecasting. MLP networks are composed of three layers named as input, hidden and output layer that are connected to each other linearly through connection weights. Consider $W^1 = \left\{ w_{ij}^1(n) \right\}$ and $W^2 = \left\{ w_{jk}^2(n) \right\}$ are the

weight matrixes which are used to link neurons of input layer to hidden ones and relate hidden layer neurons to the output one, respectively.

In order to convert output values of neurons to nonlinear ones, sigmoid function is utilized as activation function which is defined below:

$$F(x) = \frac{1}{1 + exp(x)} \tag{14.4}$$

Using the aforementioned NN, The kth output is given by:

$$y_k(n) = F\left(\sum_{j=0}^{M} w_{jk}^2(n) F\left(\sum_{i=0}^{N} w_{ij}^1(n) x_i(n)\right)\right) \tag{14.5}$$

where M and N denote the neuron number in hidden and input layer, respectively and $x_i(n)$ represents the ith input signal of nth training data.

In this chapter back propagation method is utilized to train neural network in which, MLP's estimated output value, $y_k(n)$, is compared to the desired one, $t_k(n)$, and the mean square error (MSE) value is calculated as below:

$$\begin{aligned} MSE &= \sum_{n=1}^{N} Error(n) \\ Error(n) &= \frac{1}{K} \sum_{k=1}^{K} (y_k(n) - t_k(n))^2 \end{aligned} \tag{14.6}$$

Here, n and k denote the number of training pattern and output neurons, respectively. Finally, moving in a backward direction, from output layer to input one, connection weights are modified in such a way to minimize MSE value.

In the presented method a new combination of last three years' wind speed data of Sotavento wind farm in Spain [30] is used for training MLP neural network. The important property of learning data is that other historical parameters such as pressure or temperature are not considered but the earning results were accurate enough. In the presented combination, data for each season is used as training data of that season. Totally there would be 75 inputs and 24 outputs. The input signals are 24-h wind speed of a day before prediction day, wind speed data for 24 h of the prediction day in the previous week, wind speed for all hours of prediction day in two weeks ago and the mean, maximum and minimum value of wind speed for prediction day that these last three input values are collected from weather prediction station. The output values are the 24-h wind speed of the desired prediction day.

To choose the best number for hidden layer neurons which has the least training error, neuron number in hidden layer are changed from 1 to 10 and proportional training error value is calculated for each one. Figure 14.2 depicts the proportionate training error for each number. As can be seen, 9 neurons have the least error value and it is chosen as the best neuron number of hidden layer. Neural network parameters are expressed in Table 14.1.

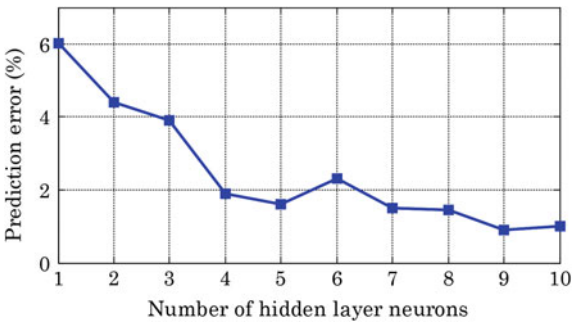

Fig. 14.2 Variation of neuron number in hidden layer and training error

Table 14.1 Neural network parameters

Neuron number in input layer	75
Neuron number in hidden layer	9
Neuron number in output layer	24
Learning factor	0.1
Learning time	2000
Transfer function	Sigmoid

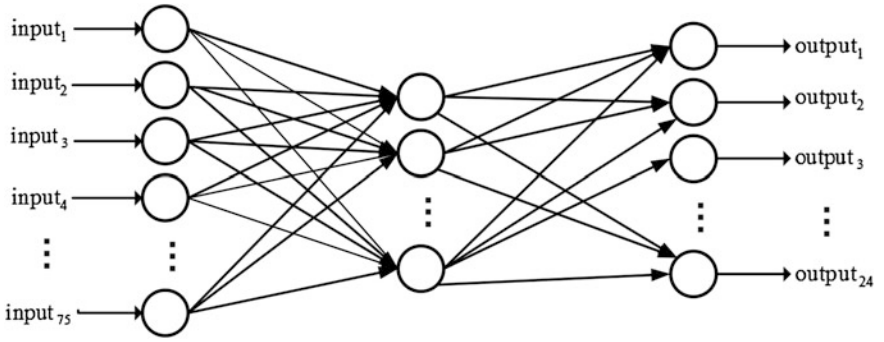

Fig. 14.3 Structure of multi-input multi-output neural network

Figure 14.3 shows the structure of a multi-input multi-output MLP neural network which is used in this work. In addition to wind speed, other uncertain parameters named above are predicted by this method too.

14.3.2 Scenario Generation Technique

Step 1. First of all, all uncertain parameters are forecasted for each hour of a 1 month period before bidding time.

Step 2. By comparing the prediction values and actual ones for the respective month, hourly error values of prediction is calculated as below:

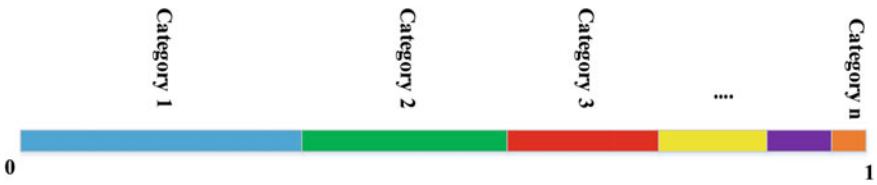

Fig. 14.4 Cumulative normalized probabilities of the prediction error categories

$$Error_t = \frac{Actual_t - Forecast_t}{Actual_t} \times 100 \tag{14.7}$$

where here $Actual_t$ and $Forecast_t$ symbolize the real and forecasted values of uncertain parameter at hour t in the respective month.

Step 3. The resulting error values proportional to each hour are classified in 1% distances while each class symbolizes a probable scenario. By dividing the frequency of each class to total month hours, occurrence probability of each error value is computed.

Step 4. In this step, the probability of categories are normalized in such a way that their total sum equals to unity. Afterward, a cumulative normalized probability is assigned to each category as shown in Fig. 14.4.

Step 5. Existence of multiple categories with various probabilities led to employ Roulette Wheel mechanism in order to generate favorite number of scenarios (here 10) for each hour. In this mechanism, a number is generated between 0 and 1, randomly and then it is compared with sorted categories. First category with cumulative probability equal or greater than random value, is selected.

Step 6. Now all of uncertain parameters are predicted for next 24 h, bidding interval, and the proportion value of each scenario is calculated as below:

$$UP_{S,t} = P_t + Error_S \times P_t \tag{14.8}$$

where $UP_{S,t}$, P_t and $Error_S$ symbolize the uncertain parameter in Sth scenario and rth hour, predicted value in hour t and prediction error in Sth scenario respectively.

Step 7. Finally, after generating desired number of scenarios, occurrence probability of each scenario is calculated as below:

$$\pi_S = \frac{\prod_{t=1}^{24} \left(\rho_{t,S}^{WT}, \rho_{t,S}^{PV}, \rho_{t,S}^{MCP}, \rho_{t,S}^{ImP}, \rho_{t,S}^{L}\right)}{\sum_{S=1}^{N_S} \prod_{t=1}^{24} \left(\rho_{t,S}^{WT}, \rho_{t,S}^{PV}, \rho_{t,S}^{MCP}, \rho_{t,S}^{ImP}, \rho_{t,S}^{L}\right)} \tag{14.9}$$

Here N_S represents total number of scenarios and $\rho_{t,S}^{WT}, \rho_{t,S}^{PV}, \rho_{t,S}^{MCP}, \rho_{t,S}^{ImP}, \rho_{t,S}^{L}$ are occurrence probability of Sth scenario of wind turbine, photovoltaic, marginal clearing price in DA market, imbalance balancing market prices and load, respectively. Flowchart of explained scenario generation process is depicted in Fig. 14.5.

In this chapter to cover all uncertainties, 10 scenario is generated for each uncertain parameter. So totally 10^5 scenarios will be existed and scenario tree for overall uncertainties is depicted in Fig. 14.6 which explains the concept of generated scenarios clearly.

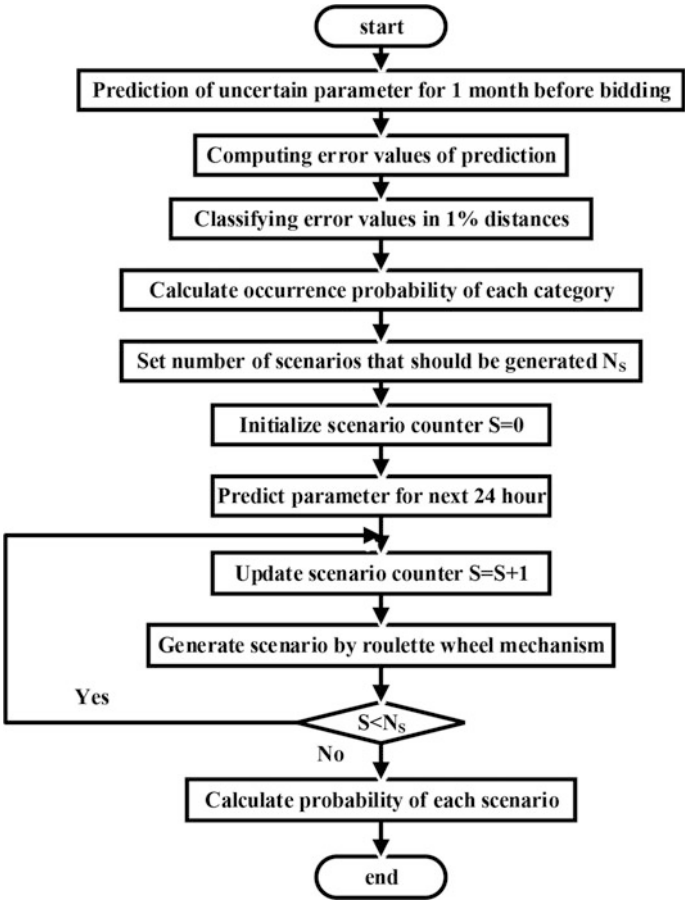

Fig. 14.5 Flowchart of scenario generation process

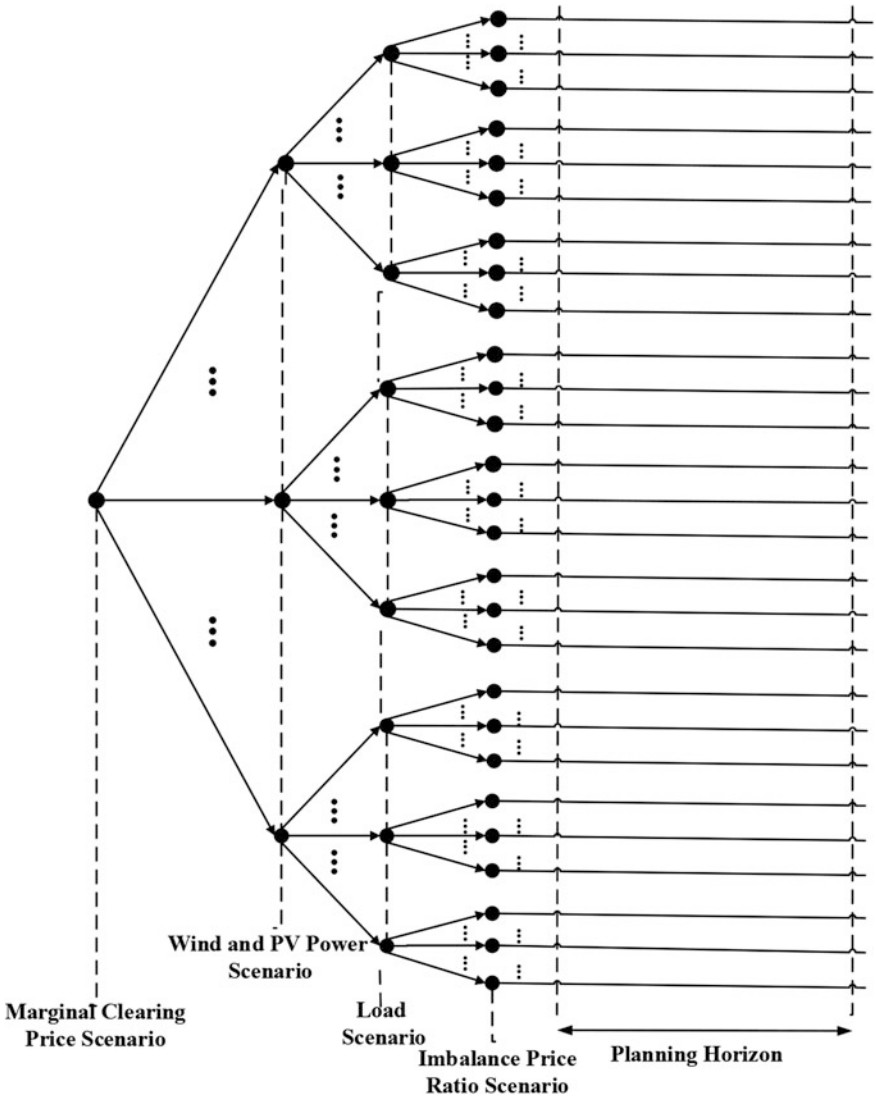

Fig. 14.6 Scenario tree of the proposed strategy

14.3.3 Scenario Reduction Technique

The aim of scenario reduction technique is to speed up optimization process. That is why in this technique some of scenarios similar to each other or the ones with very small probability of occurrence, have been omitted. Although a higher number of scenarios along with a higher computational burden can result in an accurate

modeling of the uncertainty, but a proper scenario reduction method can also approximate system's uncertain behavior efficiently. Consider S as the total set of scenarios, here 10^5, which are generated in the scenario generation process. DS symbolize the scenarios that should be omitted and is initially null. Also initialize N_D as the desired number of scenarios after reduction process. This steps of aforementioned scenario reduction process is as below:

Step 1. First of all, calculate the distance of all scenarios, two by two as below:

$$DT_{S,S'} = \sqrt{\sum_{i=1}^{d} (V_i^S - V_i^{S'})^2} \quad S, S' = 1, 2, \ldots, N_S \tag{14.10}$$

Step 2. For each scenario k, find the scenario r with least distance from scenario k as formulated below:

$$DT_{k,r} = min(DT_{k,S'}) \tag{14.11}$$

Step 3 Calculate amount of $\pi_S \times DT_{k,r}$ and elect scenario d which has the minimum production value. The election process results in selection of a scenario which has the least probability of occurrence and the most similarity to other scenarios simultaneously.

Step 4. Omit the selected scenario, $S = S - \{d\}$ and add it to omissions category, $DS = DS + \{d\}$ and also occurrence probability of d is added to its similar scenario r, $\pi_r = \pi_r + \pi_d$.

Step 5. If the favorable number of scenarios are not omitted reached, go to Step 2.

Flow chart of the explained scenario reduction process is depicted in Fig. 14.7.

14.4 Mathematical Modelling of Clean Energy Sources

The next subsections present detailed optimization formulation of abovementioned configurations. Each of these models makes effort to maximize its welfare and minimize unbalanced costs. It is worth mentioning that all equations are expressed in hourly intervals.

14.4.1 Disjoint Operation (DO)

In this operating mode, each of energy sources participate independently in power markets while aim to maximize their own income. In this mode, utilities sell their produced power to spot markets and compensate their unbalances in imbalance market. So the total income function is composed of earnings from selling power to

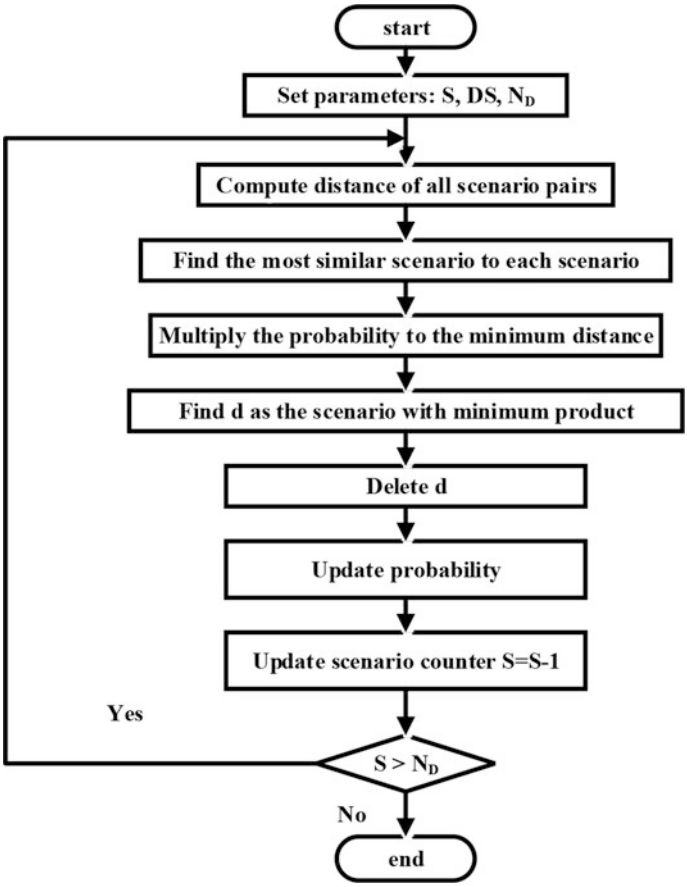

Fig. 14.7 Flowchart of scenario reduction process

day-ahead markets plus revenues from imbalance market when facing with surplus production minus penalties costs to compensate lack of committed power in imbalanced market. Welfare function related to each clean energy source along with considering its own technical constraints are formulated as below.

14.4.1.1 Wind Power Producer

Considering probable nature of available wind power, wind power producer (WPP) participate in power markets based on predicted values in scenarios but as mentioned above, scenarios are generated by forecasted wind speed values. So in order to make it possible to participate in power markets, these speed amounts must be converted to power. The relation between wind speed and power is as follow [23]:

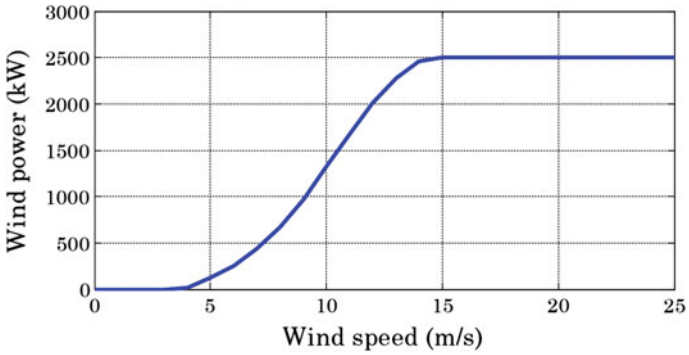

Fig. 14.8 Wind turbine power curve

$$P_{Wind} = \begin{cases} 0 & v \le v_{ci} \\ k_1 v + k_2 & v_{ci} \le v \le v_r \\ P_r & v_r \le v \le v_{co} \\ 0 & v \ge v_{co} \end{cases} \tag{14.12}$$

$$k_1 = \frac{P_r}{v_r - v_{ci}}; \quad k_2 = -k_1 \times v_{ci} \tag{14.13}$$

where v, v_{ci}, v_r and v_{co} represent the predicted wind speed, the cut-in speed of wind, the cut-out speed of wind and the wind speed at knee point of power curve, respectively. In this chapter, Nordex N80/2500 [31] which is shown in Fig. 14.8 is utilized as wind turbine power curve to transform wind speed into power.

Based on the forecasted wind power, marginal and imbalance market prices, the expected profit of wind power producer in the settlement period is described below:

$$F_{WPP} = F_{DA} + F_{Pos\_Imb} - F_{Neg\_Imb} \tag{14.14}$$

where F_{DA}, F_{Pos_Imb} and F_{Neg_Imb} are profits of day-ahead and imbalance markets and economic losses of balancing market, respectively, which are defined as follows:

$$F_{DA} = \sum_{t=1}^{24} \sum_{s=1}^{S} \rho_s \pi_{DA,t,s} P_t^{WPP} \tag{14.15}$$

$$F_{Pos\_Imb} = \sum_{t=1}^{T=24} \sum_{s=1}^{S} \rho_s \pi_{DA,t,s} \alpha_{t,s}^{+} \Delta_{t,s}^{+WPP} \tag{14.16}$$

$$F_{Neg\_Imb} = \sum_{t=1}^{T=24} \sum_{s=1}^{S} \rho_s \pi_{DA,t,s} \alpha_{t,s}^{-} \Delta_{t,s}^{-WPP} \tag{14.17}$$

The output power limits of WPP is given by:

$$0 \leq P_t^{WPP} \leq P^{W\,max} \tag{14.18}$$

$$\Delta_{t,s}^{-WPP} = P_t^{WPP} - P_{t,s}^{WPP} \tag{14.19}$$

$$\Delta_{t,s}^{+WPP} = P_{t,s}^{WPP} - P_t^{WPP} \tag{14.20}$$

$$\Delta_{t,s}^{+WPP}, \Delta_{t,s}^{-WPP} \geq 0 \tag{14.21}$$

14.4.1.2 Photovoltaic

Similar to wind power, hourly available solar energy confront with uncertainties. To manage this stochastic nature, probable solar radiation for each hour was forecasted in previous section. Now in order to calculate available solar energy, radiation must be converted to energy via underneath equation [22]:

$$P_{PV} = A_{pv}x^2 + B_{pv}x \tag{14.22}$$

While, x symbolizes the solar radiation (W/m^2), P_{PV} signifies the available solar power and A_{pv} and B_{pv} are constants which are equal to 2 and 3.6, respectively and are derived from radiation curve which is illustrated in Fig. 14.9.

Formulating profit function of photovoltaic arrays are similar to wind power producer and their both production is cost free. So, considering uncertainties of solar radiation and market prices, the profit function is contained of three terms as below:

$$F_{PV} = F_{DA} + F_{Pos\_Imb} - F_{Neg\_Imb} \tag{14.23}$$

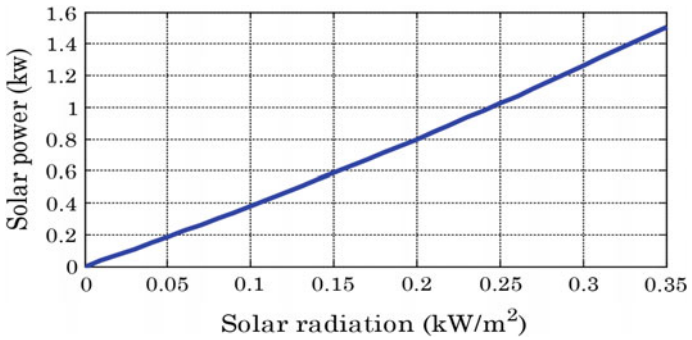

Fig. 14.9 Power-radiation curve of PV

The only difference between WPP and PV profit function is substituting solar energy instead of wind power as follow:

$$F_{DA} = \sum_{t=1}^{T} \sum_{s=1}^{S} \rho_s \pi_{DA,t,s} P_t^{PV} \tag{14.24}$$

$$F_{Pos\_Imb} = \sum_{t=1}^{T} \sum_{s=1}^{S} \rho_s \pi_{DA,t,s} \alpha_{t,s}^{+} \Delta_{t,s}^{+PV} \tag{14.25}$$

$$F_{Neg\_Imb} = \sum_{t=1}^{T} \sum_{s=1}^{S} \rho_s \pi_{DA,t,s} \alpha_{t,s}^{-} \Delta_{t,s}^{-PV} \tag{14.26}$$

Finally, the only constraint which is given here, is power limitation.

$$0 \le P_t^{PV} \le P^{PV\,max} \tag{14.27}$$

$$\Delta_{t,s}^{-PV} = P_t^{PV} - P_{t,s}^{PV} \tag{14.28}$$

$$\Delta_{t,s}^{+PV} = P_{t,s}^{PV} - P_t^{PV} \tag{14.29}$$

$$\Delta_{t,s}^{+PV}, \Delta_{t,s}^{-PV} \ge 0 \tag{14.30}$$

14.4.1.3 Demand Response

In this section mathematical formulation of demand response profit is presented. As explained before, the elasticity between MCP and demanded load has an exponential relation [21] as below:

$$Demand = ke^{\gamma \pi_{DA}} \tag{14.31}$$

where γ is a parameter to depict the relation between elasticity and market price. Participating in market, the profit of consumers equals to:

$$F_{DR} = I(D_t) - \pi_{DA} \cdot D_t \tag{14.32}$$

Equation 14.32 can be developed by Taylor series and profit function of demand side can be rewritten as:

$$F_{DR} = I\left(D_{t,s}\right) + \frac{\partial R(D_t)}{\partial D_t} \cdot \Delta D_t + \frac{1}{2} \frac{\partial^2 R(D_t)}{\partial D_t^2} \cdot (\Delta D_t)^2 - \pi_{DA} \cdot D_t \tag{14.33}$$

Substituting Eq. (14.31) with Eq. (14.33), the profit of demand side participation can be computed as:

$$F_{DR} = \sum_{t\in T}\sum_{s\in S}\rho_s((D_{t,s} - D_t) \times \pi_{DA} + \frac{1}{2} \times \frac{1}{\gamma \times D_{t,s}} \times (D_t - D_{t,s})^2) \quad (14.34)$$

Constraints of DR are as following:

$$D_t > \eta_1 \times D_{t,S} \quad \forall s \in S, \forall t \in T \quad (14.35)$$

$$D_t < (1 + \eta_2) \times D_{t,S} \quad \forall s \in S, \forall t \in T \quad (14.36)$$

Inequalities (14.35) and (14.36) define variation limits of load considering parameters η_1 and as the allowable percent of load decrease and increase. Based on (14.35) normal load level cannot decrease too much and according to (14.36) it cannot increase consumedly.

14.4.1.4 Pumped-Storage Unit

As a storage unit, pumped-storage plant conserves electricity power within low consumption and cheap hours by pumping water into top tank and releases this energy when it is needed by turbine. This process matches network delivered power to the cleared value with high accuracy.

The expected income of participating pumped-storage unit in power markets is a function of selling power $g_{t,S}^{Pump}$ to, and buying energy $d_{t,S}^{Pump}$ from, the market while considering C^{Su} and C^{Sd} as the pumping start-up and close down expenses and also two terms to cover shortage or surplus of power in balancing market. All of these functions are expressed in Eq. (14.37). Here F_{DA}, F_{Su}, F_{Sd}, F_{Pos_Imb} and F_{Neg_Imb} represent the income function in DA market, start-up and close down expenses and income and penalty in imbalance markets, respectively. Each of them are expressed in detail in Eqs. (14.38)–(14.42).

$$F_{PUMP} = F_{DA} - F_{Su} - F_{Sd} + F_{Pos\_Imb} - F_{Neg\_Imb} \quad (14.37)$$

$$F_{DA} = \sum_{t\in T}\sum_{s\in S}\rho_s \pi_{DA,t,s} P_t^{PUMP} \quad (14.38)$$

$$F_{Su} = \sum_{t\in T}\sum_{s\in S}\rho_s C^{Su} y_{t,S} \quad (14.39)$$

$$F_{Sd} = \sum_{t\in T}\sum_{s\in S}\rho_s C^{Sd} z_{t,S} \quad (14.40)$$

$$F_{Pos\_Imb} = \sum_{t\in T}\sum_{s\in S} \rho_s \pi_{DA,t,s} \alpha^{+}_{t,s} \Delta^{+PUMP}_{t,s} \tag{14.41}$$

$$F_{Neg\_Imb} = \sum_{t\in T}\sum_{s\in S} \rho_s \pi_{DA,t,s} \alpha^{-}_{t,s} \Delta^{-PUMP}_{t,s} \tag{14.42}$$

Constraints:

$$V^{U}_{t,S} = V^{U}_{t-1,S} + \eta d^{Pump}_{t,s} - g^{Pump}_{t,s} \quad \forall s \in S, \forall t \in T \tag{14.43}$$

$$V^{L}_{t,S} = V^{L}_{t-1,S} - \eta d^{Pump}_{t,s} + g^{Pump}_{t,s} \quad \forall s \in S, \forall t \in T \tag{14.44}$$

$$V^{DU} \le V^{U}_{t,S} \le V^{UU} \quad \forall s \in S, \forall t \in T \tag{14.45}$$

$$V^{DL} \le V^{L}_{t,S} \le V^{UL} \quad \forall s \in S, \forall t \in T \tag{14.46}$$

$$V^{U}_{t,S} = Vf^{U} \quad \forall s \in S, t = 1, 24 \tag{14.47}$$

$$V^{L}_{t,S} = Vf^{L} \quad \forall s \in S, t = 1, 24 \tag{14.48}$$

$$u_{t+1,S} = u_{t,S} + y_{t,S} - z_{t,S} \quad \forall s \in S, t = 1, 24 \tag{14.49}$$

$$d^{D} \cdot u_{t,S} \le d^{Pump}_{t,S} \le d^{U} \cdot u_{t,S} \quad \forall s \in S, \forall t \in T \tag{14.50}$$

$$0 \le g^{Pump}_{t,S} \le t_{t,S} \cdot g^{U} \cdot N \quad \forall s \in S, \forall t \in T \tag{14.51}$$

$$t_{t,S} \le 1 - \tfrac{1}{N} \cdot u_{t,S} \quad \forall s \in S, \forall t \in T \tag{14.52}$$

$$-d^{U} \cdot N \le P^{PUMP}_{t} \le g^{U} \cdot N \quad \forall t \in T \tag{14.53}$$

$$\Delta^{+PUMP}_{t,S} = g^{Pump}_{t,S} - d^{Pump}_{t,S} - P^{PUMP}_{t} \quad \forall s \in S, \forall t \in T \tag{14.54}$$

$$\Delta^{-PUMP}_{t,S} = P^{PUMP}_{t} - g^{Pump}_{t} + d^{Pump}_{t,S} \quad \forall s \in S, \forall t \in T \tag{14.55}$$

$$t_{t,S} \in \{0, 1\} \quad \forall s \in S, \forall t \in T \tag{14.56}$$

$$u_{t,S}, y_{t,S}, z_{t,S} \in \{0, 1, \ldots, N\} \quad \forall s \in S, \forall t \in T \tag{14.57}$$

Water balance equation in terms of energy for upper and lower reservoir is expressed in (14.43) and (14.44), in which the efficiency has an effect on the amount of energy which is pumped from bottom tank to the upper one. Equations (14.45) and (14.46) frames both reservoirs capacity limitations. Conserved energy at the end of the considered time scope is given by (14.47) and (14.48). N depicts number of identical units which form the storage unit. Also

start-up and close down expenses are taken into account in objective function by integer variables $y_{t,S}$ and $z_{t,S}$. The variable $u_{t,S}$ is allocated to the unit numbers which are functioning as turbine or pump at hour *t*. Equation (14.49) expresses the mathematical relationship between these three integer values. According to (14.50) and (14.51) pumping and turbine capacities are limited, which causes limitation on market offers (14.53). Equation (14.51) In order to prevent storage plant from operating simultaneously as a pump and turbine, binary variable t_{Sh} is defined which equals to zero in pumping mode by (14.52). Existed imbalances in each scenario and hour resulted from surplus or lack of power production are calculated by (14.54) and (14.55).

14.4.2 Joint Operation

By integration of wind power, photovoltaic, pumped storage power plant and demand response total benefit is increased in comparison to summation of individual units' profit since demand response and pumped-storage add flexibility to wind and solar power and though can complement their uncertainty. Considering above statements, microgrid profit function is formulated as below:

$$F_{PUMP} = F_{DA} - F_{Su} - F_{Sd} + F_{Pos\_Imb} - F_{Neg\_Imb} \tag{14.58}$$

$$F_{DA} = \sum_{t=1}^{T}\sum_{s=1}^{S} \rho_s \pi_{DA,t,s} P_t^{JOINT} \tag{14.59}$$

$$F_{Su} = \sum_{t=1}^{T}\sum_{s=1}^{S} \rho_s C^{Su} y_{t,S} \tag{14.60}$$

$$F_{Sd} = \sum_{t=1}^{T}\sum_{s=1}^{S} \rho_s C^{Sd} z_{t,S} \tag{14.61}$$

$$F_{Pos\_Imb} = \sum_{t=1}^{T}\sum_{s=1}^{S} \rho_s \pi_{DA,t,s} \alpha_{t,s}^{+} \Delta_{t,s}^{+JOINT} \tag{14.62}$$

$$F_{Neg\_Imb} = \sum_{t=1}^{T}\sum_{s=1}^{S} \rho_s \pi_{DA,t,s} \alpha_{t,s}^{-} \Delta_{t,s}^{-JOINT} \tag{14.63}$$

Constraints:

$$-d^U \cdot N \le P_t^{JOINT} \le P^{W\,max} + P^{PV\,max} + g^U \cdot N \quad \forall t \in T \tag{14.64}$$

$$\Delta_{t,S}^{+PUMP} = g_{t,S}^{Pump} - d_{t,S}^{Pump} - P_t^{PUMP} + D_{t,s} - D_t \quad \forall s \in S, \forall t \in T \tag{14.65}$$

$$\Delta_{t,S}^{-PUMP} = P_t^{PUMP} - g_t^{Pump} + d_{t,S}^{Pump} + D_t - D_{t,s} \quad \forall s \in S, \forall t \in T \tag{14.66}$$

In this configuration total profit is composed of 5 terms as Eqs. (14.59)–(14.63). Constraints related to joint operation is as the same as clean energy's uncoordinated operation and its difference is just in bidding limitations and imbalances calculation which are rewritten in Eqs. (14.64)–(14.66).

14.5 Simulation Results

In this part of chapter, numerical studies have been done in order to analyze joint and disjoint operation of clean energy sources and to determine bids and benefits of each configuration. To do so a test system which is composed of all these clean energy sources is considered. The proposed method has a MILP nature which is solved by CPLEX solver of GAMS software. The numerical results has been performed on a 2.3-GHz based processor with 4 GB of RAM.

14.5.1 Studied System

The schematic diagram of studied system is shown in Fig. 14.10. The case study system is composed of a 2500 kW wind turbine, solar resource with nominal power of 300 kW and two pumped-storage units with 300 and 100 kW storage and generation capacity, respectively. The wind speed data of Sotavento wind farm in Spain [30] is employed. In this chapter, annual solar radiation of Madrid, Spain which is freely available for public in SAM website [32] is utilized. The MCP is extracted from Spanish electricity market [33]. The case study is simulated for 10 February 2014. Table 14.2 shows the parameters of storage units. The start-up cost for each unit is equal to $C^{su} = 100\$$ while the close down expense is assumed to be 10$. The basic values of demand response program parameters are given in Table 14.3. Also, overall scenarios are reduced to 1000 by the aforementioned scenario reduction process.

14.5.2 Numerical Results

In this section the abovementioned method for integration of DGs is applied on a typical microgrid and numerical results are extracted. First of all it is necessary to model uncertainties and generate required scenarios. In order to analyze behavior of

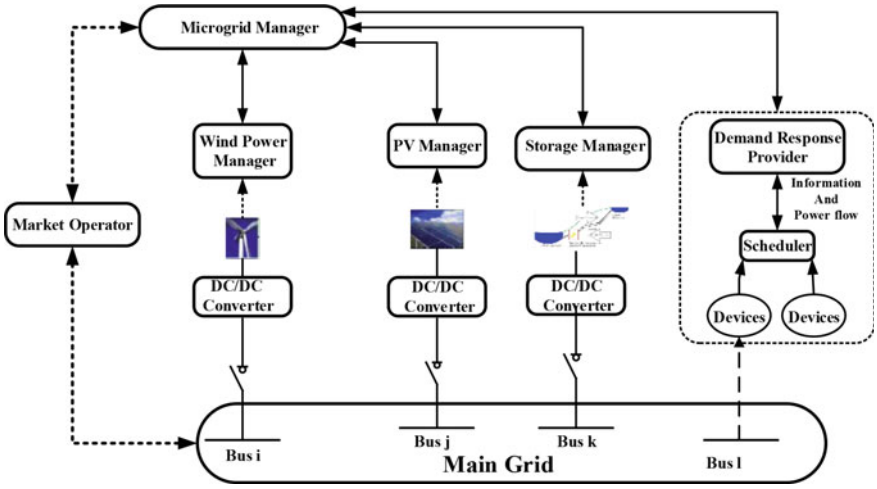

Fig. 14.10 Schematic diagram of virtual microgrid

Table 14.2 Pumped-storage characteristics

d^U (kW)	g^U (kW)	C^{su} ($)	C^{sd} ($)	η (%)	N
300	100	100	10	67	2
Upper reservoir	V^{UU} (kW)	V^{DU} (kW)		Vf^U (kW)	
	1500	0		900	
Lower reservoir	V^{UL} (kW)	V^{DL} (kW)		Vf^L (kW)	
	1500	0		900	

Table 14.3 Parameters of demand response program

Parameter	η_1	η_2	β	α
value	0.8	0.2	−0.3	0.95

imbalance market prices, hourly buy and sell imbalance prices and also hourly MCP values throughout January is extracted from [33]. Then by dividing extracted imbalance prices to their proportional MCP value, their hurly ratios are computed. In this chapter in order to demonstrate the occurrence number of ratios, box plot for ratios of buy and sell imbalance prices is depicted in Fig. 14.11. Selling power in imbalance market occurs when there is a surplus generated power with respect to the commitment. Excess of generated power will be sold cheaper than MCP and sell imbalance price ratio will be lower than unity as shown in Fig. 14.11a. On the other hand, buying imbalance power results from shortage of produced power with respect to the promised value. So it clear that this deficiency will be traded in a higher price than MCP and as can be seen in Fig. 14.11b buy imbalance price ratios will be greater than unity. Each of these buy and sell ratios are a probable scenario which can be happened.

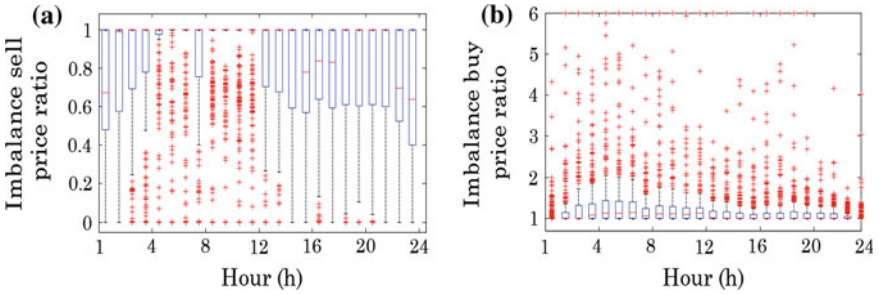

Fig. 14.11 Box plot of ratio between imbalance and marginal clearing prices

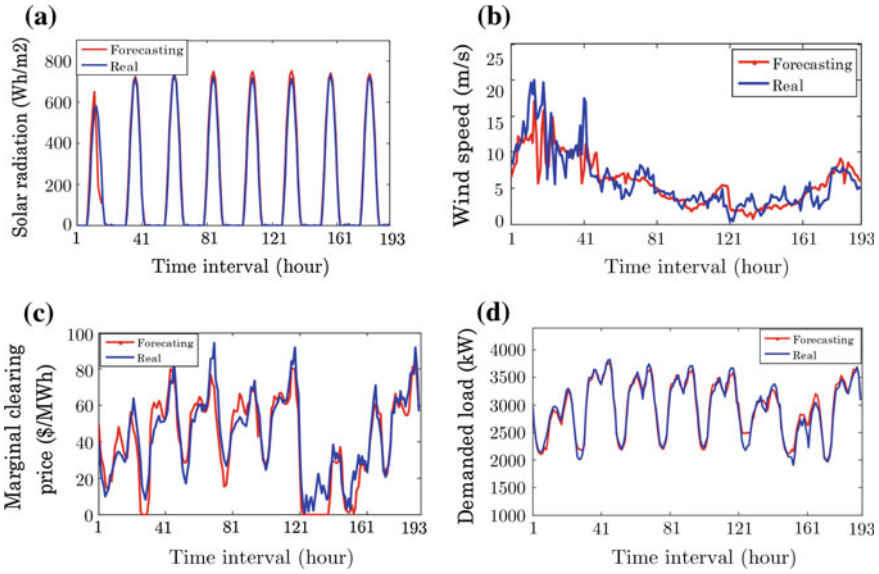

Fig. 14.12 Real and forecasted values of: **a** solar radiation, **b** wind speed, **c** marginal clearing price, and **d** demanded load

Happening probability of each these scenarios is calculated by dividing its number of occurrences to the total hours of month which equals to 720. At this point, required number of buy and sell imbalance price ratio scenarios (here 10 for each one) are generated by roulette wheel mechanism. Figure 14.12 shows the real and forecasted values of wind speed, solar radiation, MCP and load. As can be seen the prediction results are not accurate completely and there is a prediction error for most of the hours between real and forecasted values.

These error values are categorized in 1% distances for each uncertain parameter while each of these categories is considered as a probable scenario. Same as above, occurrence probability of each error value is computed by dividing its abundance to

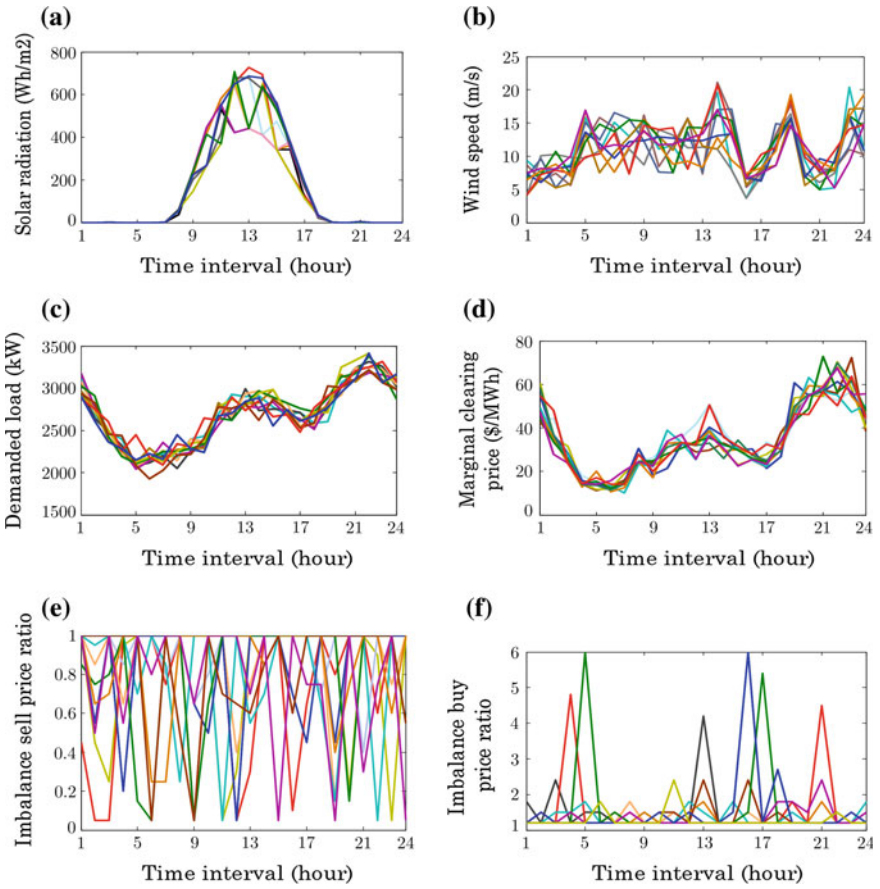

Fig. 14.13 Generated scenarios for: **a** solar radiation, **b** wind speed, **c** demanded load, **d** marginal clearing price, **e** sell imbalance price ratio and **f** buy imbalance price ratio

total number of error values. Roulette wheel mechanism is applied to generate desired number of scenarios (here 10) for each uncertain parameter. Ten generated scenarios for each of six uncertain parameters are depicted in Fig. 14.13.

The aim of optimization models is to find optimal bidding values for next day in such a way that the social welfare is maximized. In this chapter in order to explain effects of uncertainties on earned profit, optimization is done on two configurations named as disjoint and joint operation. In disjoint configuration, each of microgrid elements bid independently to maximize their own profit but in the joint operation, all of microgrid elements suggest their offers to the market by considering effects of other participants to reach the maximum profit of microgrid. Figure 14.14 depicts the optimal bidding values for each hour in these two configurations. In disjoint configuration WPP and PV offer based on their available power. As Fig. 14.14 shows PV offers only for hours between 10 till 17 while solar radiation is nonzero.

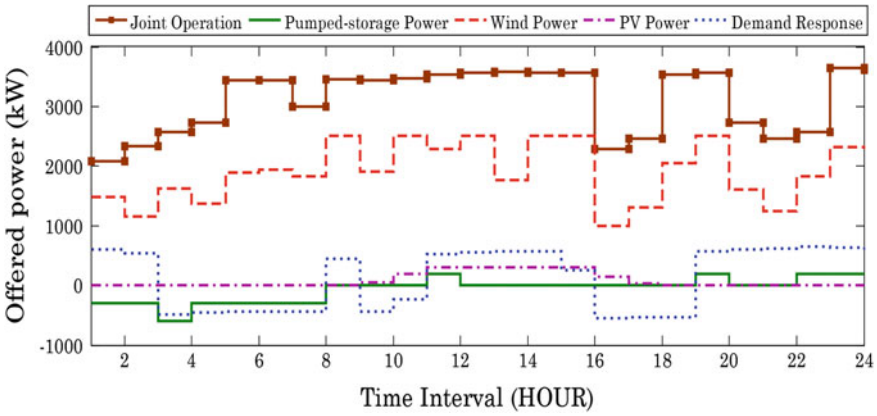

Fig. 14.14 Hourly offering quantities on 10/02/2014

Also demand response and pumped storage unit bid based on load and MCP. For example during 11 till 16 when MCP and load are high, demand response program submit its bid to reduce load but between 16 till 19 when MCP is low, it will compensate the reduced loads. On the other hand, pumped-storage unit pumps water between 1 and 8 while demanded load and MCP are low and release this energy at 11 when load is high.

By comparing the joint and disjoint operation results, it can be seen that offered power in joint mode during expensive hours is more than summation of units' individual offers because of flexibility which arises from pumped-storage plant and demand response. On the other words, during off peak and cheap hours when WPP and PV's output power is high, pumped-storage unit acts in pumping mode to store energy. To do so, it buys inexpensive power and pumps water to the upper tank in order to save energy. The stored energy is sold to earn much profit during expensive hours or to reduce penalties when WPP and PV producers face with lack of generated power because of their uncertain nature. Also, end users help this flexibility by reducing their demand during expensive hours and compensate them in cheap hours.

Numerical results related to the expected profit for each configuration is expressed in Table 14.4. WPP, PV producer, pumped-storage units and DR program earn 1663.332$, 195.957$, 367.526$ and 120$ profit when they try independently to maximize just their own profit whose summation equals to 2346.812$. But in the joint mode, integration of all units together increases overall flexibility against existence uncertainties which lead to an overall profit which equals to 2556.492$. Simulation results approve that aggregating all sources together was successful in increasing the profit by 8.9% in the case study.

This profit increase in joint mode results from hedging against solar and wind production uncertainty which is provided by pumped-storage unit and demand response via pumping water to upper reservoir and saving energy during cheap hours and releasing water and generating energy during expensive hours or by reducing consumption in costly hours and buying it in inexpensive hours.

Table 14.4 Expected profit for each configuration

Configuration		Profit ($)
DO	Wind power producer	1663.332
	PV	195.957
	Pumped-storage unit	367.526
	DR	120
	Sum	2346.815
JO		2556.492

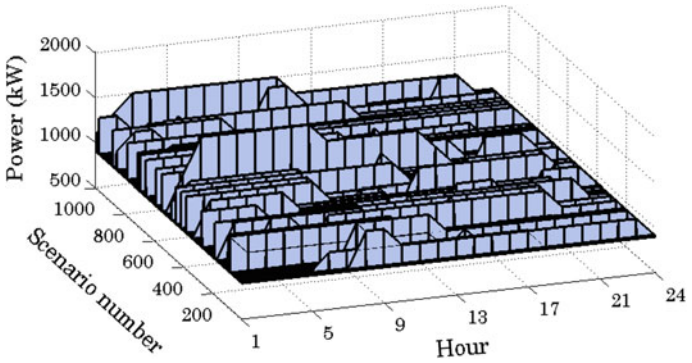

Fig. 14.15 Stored power in upper reservoir for each hour and scenario of joint operation

Figure 14.15 depicts the operation of upper reservoir of pumped-storage unit for each hour and scenario in the joint configuration. As can be seen during inexpensive hours, off-peak hours, the reservoir pumps water to its upper tank until it reaches to its upper reservoir limitation which equals to 1500 kW. Then in expensive hours it releases this energy to avoid economic losses. On the other hand, this figure proves that the initial and final value of stored energy in this reservoir equals to 900 kW which was constrained in the mathematical modeling of pumped storage unit.

14.6 Conclusion

Through this chapter, a scenario based stochastic method is proposed for planning the aggregated operation of wind turbine, photovoltaic arrays, pumped-storage unit and demand response with the goal of profit maximization. The proposed strategy considers uncertainties related to wind power, solar radiation, load, marginal and imbalance market prices over the 24 h study horizon. Using neural networks, uncertain variables are forecasted and then according to prediction errors, possible scenarios are generated and the proportional occurrence probability of each scenario is calculated. In order to save computation time, a backward scenario reduction process is applied.

The proposed four-stage-scenario-based method is tested on a typical microgrid for various operating circumstances. Numerical results approve that aggregation of all units in a microgrid can significantly increase profit value in comparison to units disjoint operation. The results also approve that, demand response and pumped-storage plant as storage devices can efficiently cover production power uncertainties of microgrid units and make wind and solar producers more competitive in day-ahead power markets. On the other hand, by considering uncertainties of negative/positive imbalance market prices and marginal prices of day-ahead market, more probable prices are considered.

References

1. Shi L, Luo Y, Tu GY (2014) Bidding strategy of microgrid with consideration of uncertainty for participating in power market. Int J Electr Power Energy Syst 59:1–13
2. Niknam T, Azizipanah-Abarghooee R, Narimani R (2012) An efficient scenario-based stochastic programming framework for multi-objective optimal micro-grid operation. Appl Energy 99:455–470
3. Lidula NWA, Rajapakse AD (2011) Microgrids research: a review of experimental microgrids and test systems. Renew Sustain Energy Rev 15:186–202
4. Blaabjerg F, Chen Z, Kajaer SB (2004) Power electronics as efficient interface in dispersed power generation systems. IEEE Trans Power Electr 19(5):1184–1194
5. Rocabert J, Luna A, Blaabjerg F et al (2012) Control of power converters in AC microgrids. IEEE Trans Power Electr 27(11):4734–4749
6. Katiraei F, Iravani R, Hatziargyrious N et al (2008) Microgrids management. IEEE Power Energy Mag 6(3):54–65
7. Eghtedarpour N, Farjah E (2014) Power control and management in a hybrid AC/DC microgrid. IEEE Trans Smart Grid 5(3):1494–1505
8. Anbazhagan S, Kumarappan N (2014) Day-ahead deregulated electricity market price forecasting using neural network input featured by DCTO. Energy Convers Manage 78:711–719
9. Sharma KC, Bhakar R, Tiwari HP (2014) Strategic bidding for wind power producers in electricity markets. Energy Convers Manage 86:259–267
10. Koo J, Han GD, Choi HJ et al (2015) Wind-speed prediction and analysis based on geological and distance variables using an artificial neural network: a case study in South Korea. Energy 93:1296–1302
11. Pousinho HMI, Mendes VMF, Catalao JPS (2011) A hybrid PSO-ANFIS approach for short term wind power prediction in Portugal. Energy Convers Manage 52:397–402
12. Shayeghi H, Ghasemi A (2013) Day-ahead electricity prices forecasting by a modified CGSA technique and hybrid WT in LSSVM based scheme. Energy Convers Manage 74:482–491
13. Zuluaga CD, Alvarez MA, Giraldo E (2015) Short-term wind speed prediction based on robust Kalman filtering: an experimental comparison. Appl Energy 156:321–330
14. Shayeghi H, Ghasemi A, Moradzadeh M et al (2015) Simultanous day-ahead forecasting of electricity price and load in smart grids. Energy Convers Manage 95:371–384
15. Pousinhoa HMI, Mendesc VMF, Catalo JPS (2012) A stochastic programming approach for the development of offering strategies for a wind power producer. Electr Power Syst Res 89:45–53
16. Shayeghi H, Hashemi Y (2015) Application of fuzzy decision-making based on INSGA-II to designing PV-wind hybrid system. Eng Appl Artif Intell 45:1–17

17. Shayeghi H, Bagheri A (2013) Dynamic sub-transmission system expansion planning incorporating distributed generation using hybrid DCGA and LP technique. Int J Electr Power Energy Syst 48:111–122
18. García-González J, de la Muela RMR, Santos LM et al (2008) Stochastic joint optimization of wind generation and pumped-storage units in an electricity market. IEEE Trans Power Syst 23 (2):460–468
19. Karimi Varkani A, Daraeepor A, Monsef H (2011) A new self-sceduling strategy for integrated operation of wind and pumped-storage power plants in power markets. Appl Energy 88:5002–5012
20. Parastegari M, Hooshmand RA, Khodabakhshian A et al (2013) Joint operation of wind farms and pump-storage units in the electricity markets: Modeling, simulation and evaluation. Simul Model Pract Theor 37:56–69
21. Mohammadi J, Rahimi-Kian A, Ghazizadeh MS (2011) Aggregated wind power and flexible load offering strategy. IET Renew Gener 5:439–447
22. Mohammadi M, Hosseinian SH, Gharehpetian GB (2012) Optimization of hybrid solar energy sources/wind turbine systems integrated to utility grids as microgrid (MG) under pool/bilateral/hybrid electricity market using PSO. Sol Energy 86:112–125
23. Mohammadi S, Soleymani S, Mozafari B (2014) Scenario-based stochastic operation management of MicroGrid including wind, photovoltaic, micro-turbine, fuel cell and energy storage devices. Int J Electr Power Energy Syst 54:525–535
24. Sortomme E, El-Sharkawi MA (2009) Optimal power flow for a system of microgrids with controllable loads and battery storage. In: IEEE/PES Power System Conference, pp 1–5
25. Shayeghi H, Sobhani B (2014) Integrated offering strategy for profit enhancement of distributed resources and demand response in microgrids considering system uncertainties. Energy Convers Manage 87:765–777
26. Alharbi W, Raahemifar K (2015) Probabilistic coordination of microgrid energy resources operation considering uncertainties. Electr Power Syst Res 128:1–10
27. Aghajani GR, Shayanfar HA, Shayeghi H (2015) Presenting a multi-objective generation scheduling model for pricing demand response rate in micro-grids energy management. Energy Convers Manage 106:308–321
28. Motevasel M, Seifi AR (2014) Expert energy management of a microgrid considering wind energy uncertainty. Energy Convers Manage 83:58–72
29. Chen C, Duan S, Cai T et al (2011) Smart energy management system for optimal microgrid economic operation. IET Renew Power Gen 5:258–267
30. http://www.sotaventogalicia.com/index.php
31. Nordex N80/2500 wind turbine catalogue. http://www.nordex-online.com/en/produkte-service/wind-turbines/n80-25-mw.html
32. http://www.solargis.info
33. http://www.esios.ree.es/web-publica/